Journal of Sciences, Islamic Republic of Iran 31(3): 233 - 244 (2020) http://jsciences.ut.ac.ir
University of Tehran, ISSN 1016-1104

Kinetic Modelling of Methanol to Propylene Process on Cerium-hierarchical SAPO-34 Catalyst

M. Ghalbi-Ahangari[1*], A. Taheri Najafabadi[2], P. Rashidi-Ranjbar[2], Z. Taheri[1]

[1] *Research Institute of Petroleum Industry (RIPI), P.O. Box 14665-1998, Tehran, Islamic Republic of Iran*
[2] *Department of Chemistry, Faculty of Sciences, University of Tehran, Tehran, Islamic Republic of Iran*

Received: 18 February 2020 / Revised: 13 Apr 2020 / Accepted: 11 May 2020

Abstract

In this paper, conventional SAPO-34 and Cerium Hierarchical SAPO-34 zeolites are synthesized using a hydrothermal method for methanol-to-propylene (MTP) reaction. The Ce-H-SAPO-34 catalyst shows a slightly larger crystal size, bimodal pore size distribution (microporous and mesoporous) and lower surface acidity compared to conventional SAPO-34 catalysts. According to these physicochemical properties and the previously suggested reaction mechanisms on the conventional SAPO-34 catalyst, a new reaction network is introduced for Ce-H-SAPO-34 catalyst. This was based on the data collected from a catalytic micro reactor in the temperature range of 390-450°C and at atmospheric pressure. The lumped kinetic model and the reaction rate expression have been introduced by considering the reaction network. The parameters were then estimated based on the experimental data using genetic algorithms. Comparing the experiments with the predicted data suggests a good correlation between the experimental data and the model.

Keywords: Kinetic modeling; Methanol to propylene process; Lumped kinetic model; Ce-H-SAPO-34.

Introduction

Propylene, with a chemical formula of $CH_3CH=CH_2$, undoubtedly is one of the oldest and earliest raw materials which is mainly used for polypropylene production. Also, some other petrochemical industries which produce Cumene, Oxo alcohols, propylene oxide and acrylonitrile are using propylene as feedstock. The propylene increasing demand in the international market and decreasing oil resources as the main route of propylene production, lead to developing processes with reasonable propylene productivity [1-3]. The methanol to olefins (MTO) process, which was commercialized by UOP/Hydro and the methanol to propylene (MTP) process, which was developed by Lurgi, are known as two interesting alternative sources for propylene production that are not dependent to oil resources.

The MTO process utilizes a SAPO-34 catalyst that promotes a high selectivity toward ethylene and propylene as light olefins (>80 %). This molecular sieve has an 8-membered ring with a narrow pore opening (0.38 nm × 0.38 nm) and large CHA cages. One of the most common disadvantages of this catalyst is the high amount of coke formation, which is trapped into SAPO-34 cages and leads to quick catalyst deactivation. Therefore the MTO process requires a fluidized bed

* Corresponding author: Tel: +982148255072; Fax: +982144739752; Email: ahangarym@ripi.ir

reactor [4].

In contrast, the MTP process uses a ZSM-5 zeolite in a fixed bed reactor. This catalyst has a three-dimensional 10-membered ring channels; Some micro pores (0.51 nm × 0.55 nm) exists in a zigzag channels parallel to plane (100) and some others (0.53 nm × 0.56 nm) appears in straight channels parallel to plane (010) in a MFI framework. The unique structure and surface acidity of this catalyst leads to high propylene-to-ethylene (P/E) ratio in the process; therefore the above process predominantly produces propylene [5-7].

Some modifications have been applied to the SAPO-34 catalyst in methanol to olefin reaction, to inhibit the rapid catalyst deactivation and to improve propylene selectivity. These modifications follow some strategies like tuning of acid sites, reducing the zeolite crystal dimensions and applying some tailored additives to improve the productivity of the process [8, 9]. The reduction of the diffusion barrier is another technique that can be applied by introducing mesoporosity during the hydrothermal synthesis of zeolite crystals, to achieve a hierarchical structure [10, 11]. In most SAPO-34 catalyst cases, the hierarchical structure is known as a bimodal pore system (mesoporous and microporous), which showed superior performance in comparison with conventional ones [11-13]. Besides, the presence of mesopores in the hierarchical SAPO-34 provides a proper site for deposition of metals and metal oxides as new active sites. The impregnation of SAPO-34 with metal particles may lead to modified material with different textural properties such as profound changes in acidic characteristics [14, 15].

It is essential in the petrochemical industry to evaluate the performance of this catalytic process (i.e. methanol conversion and propylene selectivity). It seems that the kinetic models of the MTO/MTP process could be necessary for MTO/MTP reactor design, modeling and processes optimization in the initial commercial evaluation. Such kinetic models applied in the simulation of various types of reactors to estimate product distribution and to determine the reactor dimensions [16]. Few researchers focused on MTO/MTP reaction pathway and its related kinetic model. The reaction network of the methanol conversion to olefins is very complex and most of the researchers had not been considered the reaction intermediates. They had developed lumped kinetic models based on "Hydrocarbon pool" mechanism [17-19]. In the suggested mechanism, DME and methanol instantly reach to equilibrium, over the surface of the catalyst. Therefore both of them can contribute as a feedstock to produce various types of hydrocarbons. This carbon pool is repeatedly building up and breaking down to yield methane, lower molecular weight olefins ($C_1^=$-$C_5^=$) and coke.

Gayubo et al. [20] studied a lumped kinetic model to predict the formation of light olefins from methanol on a SAPO-18 catalyst in a variety range of operating conditions. That kinetic model proposed three consecutive steps that change with reaction time. The active intermediate compounds were created in the first step (initiation period) of the reaction. The latter steps are olefin production and deactivation process, respectively. They examined several reaction networks to find out the reaction pathways. Some of these reaction pathways suggested the connection of lighter olefins species in the hydrocarbon pool to form higher molecular weight olefins. The other reaction network assumed the direct reaction of methanol/DME with intermediate compounds in the hydrocarbon pool for the formation of different kinds of olefins. There was no significant difference between these two proposed models. In another try, a seven lumped kinetic model was developed by Aguayo et al. [21] to express the methanol to hydrocarbon reaction (MTH) product distribution over a high acidic HZSM-5 zeolite. Their recommended kinetic model fitted well the experimental data which was acquired at 400–550 °C temperature range in a catalytic fixed bed reactor. The methanol retention time in the reactor was varied during the kinetic study to obtain different methanol conversion and its effects on the product distribution. Also, Taheri Najafabadi et al. [22] presented a new ten lumped kinetic model for methanol to olefins process on the fresh SAPO-34 catalyst by use of a suitable reaction network. Their experimental data was acquired from a catalytic micro reactor in three different reactor temperatures (400, 425 & 500ºC) and three different methanol space time (0.86, 1.69 & 2.98 (gcat. h/mol MeOH)). The proposed kinetic model had an excellent capability for the prediction of conventional SAPO-34 catalyst performance.

Most of the previous lumped kinetic models for MTH, MTO and MTP processes, were suitable for predictions of the performance of SAPO and ZSM5 catalysts with narrow entrance pore. The effects of the pores structure on the reaction pathway and its related kinetic models have not been investigated in any researches until yet.

In the present study, the cerium impregnated hierarchical SAPO-34 catalyst was synthesized using n-propylamine (NPA) and Cerium nitrate for the MTP process. The kinetic model was studied on the Ce-H-SAPO-34 catalyst in an integral fixed bed reactor. The methanol to olefin process reaction network on conventional SAPO-34 catalyst which was introduced

by [22], has been modified to find out new reliable and straightforward reaction pathways on Cerium promoted Hierarchical SAPO-34 catalyst. By considering reaction mechanism, the equation of reaction rates was introduced, and the reaction rate parameters (i.e. pre-exponential factors and activation energy) were estimated by genetic algorithm.

Materials and Methods

Materials

Ortho-phosphoric acid (H_3PO_4, 85 wt%), methanol (MeOH, 99.9%) and Tetraethyl ammonium hydroxide (TEAOH, 20wt.% aqueous solution) all purchased from Merck and have been used without any further purification. Fumed silica (FS, 98 wt.%), Aluminum isopropoxide (AIP, 97 wt.%) and n-propylamine (NPA, 99 wt.%) purchased from Aldrich and have been utilized without extra process.

Methods

Catalyst preparation

The hierarchical SAPO-34 was prepared hydrothermally based on our previous work [14]. A special amount of aluminum isopropoxide dissolved in deionized water and then ortho-phosphoric acid was added to the prepared solution dropwise and stirred for 30 minutes. After the time, fumed silica was added continuously to the solution while the mixture was stirring to get a homogeneous solution. Then TEAOH and NPA were added until a gel was formed. The resulting gel was kept at room temperature for 24 h to become hydrolyzed and then transferred into stainless steel Teflon-lined autoclaves for hydrothermal treatment at 200 ºC for 12 h. The resulted crystals were washed several times and recovered by centrifugation and then dried at 120ºC and calcined at 550ºC for 6 h to remove the organic components.

The Ce-H-SAPO-34 catalyst was prepared using additional processes of the H-SAPO-34 suspension in diluted cerium nitrate solution and stirring the mixture to impregnate the hierarchical SAPO-34. Then the catalyst filtered, dried at 120ºC and calcined at 550ºC for 6h.

Catalyst characterization

The prepared SAPO-34 catalysts X-ray spectra were taken using PHILIPS-PW1840 diffractometer with monochromatized Cu-Kα radiation operated at 25 mA and 40 kV. The scans were recorded in the 2θ range between 1° and 50° using the scanning rate of 3º/min. The Scanning electron microscopy (SEM) was performed on the prepared catalysts using a Philips XL30 machine to discover the catalyst particle morphology. The synthesized catalysts surface area and its pore size distribution were measured by N_2 adsorption-desorption isotherms at liquid nitrogen temperature (77 K). The tests were carried out using a Micromeritics 3020 apparatus in a relative pressure ranged from 0.02 to 0.99. Before the measurement, the catalysts were degassed under the vacuumed condition at 200ºC for 2 hr. Brunauer–Emmett–Teller (BET) model was used to evaluate the total surface area. Each sample total pore volume was estimated from the amount of N_2 adsorbed at a relative pressure of 0.99. The micropore volume was determined from the Dubinin-Radushkevich equation (DR) and t-plots as described in [13, 14]. The difference between the total pore volumes and micropore volume give estimation for mesopore volume. NH_3-TPD was examined using Micrometritics 2900 TPD/TPR device. 100 mg of calcined samples were first degassed for 1 h under 20 mL/min helium flow at 400 ºC and then cooled to 100ºC. After that the mentioned sample was saturated with NH_3 using a dilute stream of NH_3 in helium for 1 h. The gas mixture was then altered to Helium, and the sample was purged at 100ºC for 1 h to remove any molecules of ammonia, which already has been adsorbed physically on the catalyst surface. In the final step, the catalyst bed temperature was increased by a 10ºC/min heating rate from 100 to 650 ºC in a constant helium flow. The desorbed NH_3 was recorded by a TCD and was depicted as a function of temperature.

Packed bed reactor

The experiments performed in a fixed bed Pyrex reactor (50 cm high and 1.1cm internal diameter) at atmospheric pressure. In each experimental run, 1g of the prepared catalyst with mesh size 20-40, was loaded at the center of reactor. An electrical jacket around the reactor provided the heat transfer media. The reaction temperature measured by a thermocouple near the catalyst bed center and was controlled by a PID controller.

The methanol feed was mixed with water, then both evaporated and passed downwards through the catalyst bed with an additional flow of N_2 (60 mL/min) as dilatants gas. This procedure helped to reduce the catalyst deactivation rate and to increase selectivity towards lower olefins. The temperature ranges of 390 to 450 ºC were examined to evaluate the catalyst performance at three different methanol space velocities.

When steady-state conditions reached in any experimental run, a portion of the gas mixture that already left the reactor, was analyzed using an on-line

GC (Agilent 6890 gas chromatograph) equipped with TCD and FID detectors and PONA and Al_2O_3 capillary columns.

Results and Discussion

Catalyst characterization

The X-ray spectra of the synthesized catalysts were plotted in Figure 1. The SAPO-34 specific peaks with a small increase in the peak sharpness appeared in the XRD pattern of cerium impregnated hierarchical SAPO-34. Therefore, the cerium oxide species did not disturb the SAPO-34 crystalline framework. Also, the cerium oxide species correspondent reflections were not detected in the X-ray diffraction patterns of Ce-H-SAPO-34 catalyst. This phenomenon may happen when the cerium oxide species homogeneously dispersed on the surface of the hierarchical SAPO-34 catalyst. This would be intensified when the cerium content is too much low [23].

Figure 2 illustrated the SEM images of SAPO-34 and Ce-H-SAPO-34 catalysts. Both of the samples show the characteristic cubic morphology of the CHA crystals [24], except that the particle size distribution of Ce-H-SAPO-34 is narrower than the conventional SAPO-34 catalyst. The BET surface area for Ce-H-SAPO-34 catalyst is lower than the conventional SAPO-34 catalyst, as presented in Table 1, but the mesoporosity of Ce-H-SAPO-34 is much higher and this catalyst showed a bimodal pore size distribution.

The NH_3-TPD results were presented in Table 2.

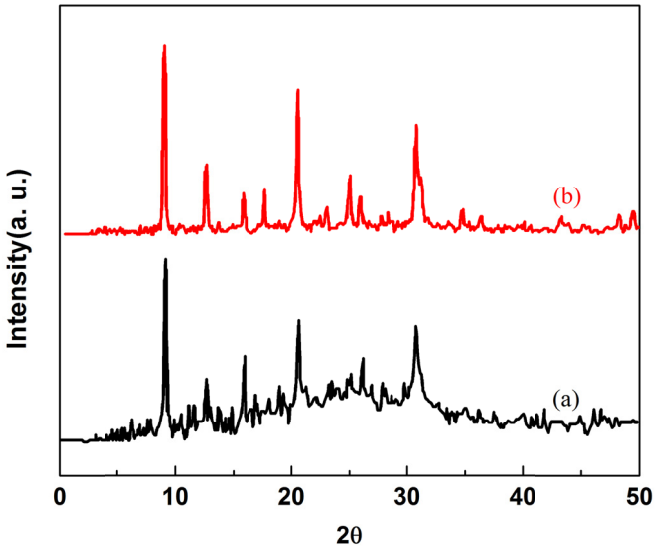

Figure 1. X-ray spectra of (a) conventional SAPO-34, (b) Cerium impregnated hierarchical SAPO-34

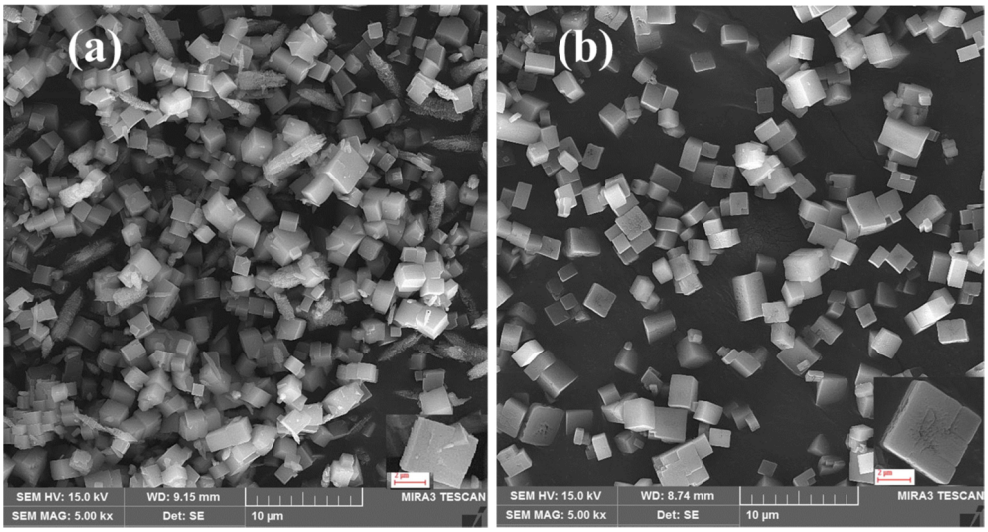

Figure 2. SEM images of (a) conventional SAPO-34 and (b) Cerium impregnated hierarchical SAPO-34

Two main peaks around 200˚C and 400˚C were detected in both SAPO-34 and Ce-H-SAPO-34 catalysts. These two desorption peaks were attributed to the weak and strong acidic sites, respectively. The quantitative amounts of both acidic sites in Ce-H-SAPO-34 catalyst were lower compared to the conventional SAPO-34 [25]. Therefore this catalyst showed a moderate acidity compared to SAPO-34 catalyst.

Kinetic study

With respect to the reliable reaction network for MTO process, Taheri Najafabadi et al. [22] had developed a new lumped kinetic model. That kinetic modeling study performed based on data obtained on the common microporous SAPO-34 catalysis. The Hierarchical SAPO-34 in present work has a bimodal pore structure (mesoporous and microporous) with lower acidity compared to common micro porous SAPO-34 catalyst. Changing the catalyst structure and its surface properties might change the reaction path and product distribution.

Based on the Cerium promoted H-SAPO-34 catalyst characteristics compared to common SAPO-34, a new 12 reaction networks were presented in Table 3. In the first reaction steps, methanol and dimethyl ether quickly reached to equilibrium on the surface of the synthesized catalyst, before the initiation reaction for the production of any other hydrocarbon started [20, 21, 26]. Both methanol and DME may contribute to the production of Ethylene as a primary product. After that the already produced DME and reactant methanol acted as methylation agents and continuously combined with lighter olefins ($C_1^=$-$C_2^=$) in the hydrocarbon pool to form higher molecular weight olefins ($C_3^=$-$C_5^=$) [26-30]. Therefore, the reactions 3-6 have been introduced to the reaction network in Table 3.

For conventional microporous SAPO-34 catalysts with strong acidity, the main portion of methanol would convert to ethylene and no more methanol present in the hydrocarbon pool to react successively with lower olefins [28, 30]. Commonly, the DME is considered as a dominant species for methylation agents in the hydrocarbon pool [30]. For Ce-Hierarchical SAPO-34 catalyst of the present study with moderate acidity and lower hydrocarbon cracking potential, it is supposed that both methanol and DME may participate in the hydrocarbon pool to make higher molecular weights olefins. Based on this assumption, for the first time, two

Table 1. The BET and pore volumes of conventional SAPO-34 and Cerium impregnated hierarchical SAPO-34

Sample	BET Surface Area (m^2/g)	Total Pore Volume (m^3/g)	Micropore volume (m^3/g)	Mesopore volume (m^3/g)
SAPO-34	605.1	0.14	0.12	0.02
Ce-H-SAPO-34	364.4	0.27	0.09	0.18

Table 2. Ammonia TPD results of SAPO-34 and Cerium impregnated hierarchical SAPO-34

Catalyst	Peak temperature (°C)		NH_3 Desorbed (mmol/g)	
	Low Temp.	High Temp.	Weak sites	Strong sites
SAPO-34	198	398	1.48	1.77
Ce-H-SAPO-34	174	380	0.95	0.99

Table 3. The new reaction network

$\boldsymbol{2MeOH \overset{K_{r1}}{\Leftrightarrow} [(CH_3)_2O] + H_2O}$	(1)
$2[(CH_3)_2O] \overset{k_{r2}}{\rightarrow} C_2H_4 + 2\,MeOH$	(2)
$2MeOH \overset{k_{r3}}{\rightarrow} C_2H_4 + 2H_2O$	(3)
$C_2H_4 + DME \overset{k_{r4}}{\rightarrow} C_3H_6 + MeOH$	(4)
$C_2H_4 + MeOH \overset{k_{r5}}{\rightarrow} C_3H_6 + H_2O$	(5)
$C_3H_6 + DME \overset{k_{r6}}{\rightarrow} C_4H_8 + MeOH$	(6)
$C_3H_6 + MeOH \overset{k_{r7}}{\rightarrow} C_4H_8 + H_2O$	(7)
$C_4H_8 + DME \overset{k_{r8}}{\rightarrow} C_5H_{10} + MeOH$	(8)
$MeOH \overset{k_{r9}}{\rightarrow} CO + 2H_2$	(9)
$CO + H_2O \overset{k_{r10}}{\rightarrow} CO_2 + H_2$	(10)
$MeOH + H_2 \overset{k_{r11}}{\rightarrow} CH_4 + H_2O$	(11)
$C_2H_4 + H_2 \overset{k_{r12}}{\rightarrow} C_2H_6$	(12)

new reactions were added to the reaction network proposed by [22] for predicting the Ce-Hierarchical SAPO-34 catalyst performance in the MTP process. A twelve elementary reaction rate expression were presented with respect to the supposed reaction network. All 24 kinetic parameters related to these reaction rates in Table 4, estimated through the experimental data in the fixed bed reactor. Gayubo et al. [26] suggested reaction equilibrium constant (K) for methanol conversion to DME on ZSM-5 catalyst based on detailed experimental data as follows:

$$-R.\ln K_p = \frac{\Delta G}{T} = -\frac{4163}{T} + 2\ln T - 1.01\times10^{-3}T - 5.82\times10^{-6}T^2 - 10.76 \quad (1)$$

All the reactions in Table 3 assumed to be an elementary reaction. So their orders in Table 4 could be found from their stoichiometric coefficient in the reaction. Bos et al. [27] proved that the reaction orders for the production of ethylene from DME (R-2) and methanol (R-3) are 1. This result also certified by Taheri Najafabadi et. al [22]

Experimental data on Ce-H-SAPO-34

The experiments were performed in three temperatures, i.e. 390°C, 420°C and 450°C. Also, in each specific temperature, three different feed (methanol/water) residence times were applied. The data were gathered after 30 minutes reaction and is shown in Table 5. It was assumed that no cokes formed inside the pores of the Ce-H-SAPO-34 catalyst at this period.

Parameter Estimation Procedure

By performing the mass balance for each chemical compound based on the proposed reaction network, a comprehensive reactor model was obtained. The component molar flow (Fi) at the reactor outlet was computed from the following continuity equations assuming plug flow in the fixed bed experimental reactor:

$$\frac{dF_i}{dW} = \sum r_i \qquad i = 1,2,...,n \quad (2)$$

$$C_i = C_{T0}\frac{F_i}{F_T}\times\frac{P}{P_0}\times\frac{T_0}{T} \qquad F_T = \sum_{i=1}^{n} F_i \quad (3)$$

In this equation:

F_i: Component i molar flow rate inside reactor(mole/min)

W: The catalyst amount in reactor, g

$\sum r_i$: Net production rate of each component based on components concentration

Table 4. Reaction rate equation for MTP process

$\boldsymbol{r_1 = k_{01}.\exp(-\frac{E_1}{RT}).C_{MeOH}{}^2 - \frac{k_{01}}{K}.\exp(-\frac{E_1}{RT}).C_{DME}.C_{H_2O}}$	(1)
$r_2 = k_{02}.\exp(-\frac{E_2}{RT}).C_{DME}$	(2)
$r_3 = k_{03}.\exp(-\frac{E_3}{RT}).C_{MeOH}$	(3)
$r_4 = k_{04}.\exp\left(-\frac{E_4}{RT}\right).C_{DME}.C_{C_2H_4}$	(4)
$r_5 = k_{05}.\exp\left(-\frac{E_5}{RT}\right).C_{MeOH}.C_{C_2H_4}$	(5)
$r_6 = k_{06}.\exp\left(-\frac{E_6}{RT}\right).C_{DME}.C_{C_3H_6}$	(6)
$r_7 = k_{07}.\exp\left(-\frac{E_7}{RT}\right).C_{MeOH}.C_{C_3H_6}$	(7)
$r_8 = k_{08}.\exp\left(-\frac{E_8}{RT}\right).C_{DME}.C_{C_4H_8}$	(8)
$r_9 = k_{09}.\exp(-\frac{E_9}{RT}).C_{MeOH}$	(9)
$r_{10} = k_{10}.\exp\left(-\frac{E_{10}}{RT}\right).C_{CO}.C_{H_2O}$	(10)
$r_{11} = k_{11}.\exp\left(-\frac{E_{11}}{RT}\right).C_{MeOH}.C_{H_2}$	(11)
$r_{12} = k_{12}.\exp\left(-\frac{E_{12}}{RT}\right).C_{MeOH}.C_{C_2H_4}$	(12)

Table 5. Experimental data gathered from integral fixed bed reactor used for reaction rate parameter estimation

T(°C)	390	390	390	420	420	420	450	450	450
Components Flow in Reactor Inlet (mol/min) *10^{-3}									
CH_3OH	23.16	29.37	35.21	23.16	29.37	35.21	23.16	29.37	35.21
H_2O	24.80	18.33	12.66	24.80	18.33	12.66	24.80	18.33	12.66
Components Flow in Reactor Outlet (mol/min)*10^{-3}									
CH_4	0. 11	0. 17	0. 38	0. 14	0. 19	0. 44	0. 16	0. 22	0. 52
C_2H_4	2.80	3.70	4.60	2.90	3.80	4.80	3.10	3.90	4.90
C_2H_6	0. 17	0. 2	0. 32	0. 18	0. 2	0. 33	0. 19	0. 22	0. 35
C_3H_6	3.10	4.30	4.90	3.30	4.50	5.00	3.40	4.60	5.10
C_3H_8	0. 3	0. 38	0. 45	0. 33	0. 45	0. 45	0. 34	0. 46	0. 46
C_4H_8	0. 34	0. 45	0. 58	0. 35	0. 45	0. 62	0. 37	0. 47	0. 64
C_4H_{10}	0. 44	0. 43	0. 41	0. 36	0. 24	0. 24	0. 21	0. 11	0. 1
C_5H_{10}	0.24	0.25	0.29	0.24	0.28	0.29	0.25	0.28	0. 31
CH_3OH	0.077	0.057	0.033	0.069	0.041	0.022	0.042	0.021	0.011
DME	0.068	0.063	0.045	0.052	0.038	0.018	0.031	0.017	0.011
H_2O	0.11	0.28	0.35	0.45	0.57	0.66	0.46	0.66	0.81
H_2	0.16	---	0.28	0.49	0.41	0.66	---	0.35	0.13
CO_2	0.99	0.65	0.42	0.41	0.28	0.15	0.21	0.14	0.10

C_{T0}, P_0, T_0: Total concentration, Pressure and Temperature at the reactor inlet

The sets of differential equations should be solved simultaneously to predict the reactor outlet. The Gear's method was applied to solve these differential equations numerically. The zero product flow rates at the surface of the catalyst bed were assumed to be the initial condition. The reactor products were compared with experimental data and the objective function was calculated based on the previous experiences expressed by [28, 30-32]. The proposed objective function was the absolute relative deviation of calculated data from experimental data.

$$OF = \frac{1}{m}\sum_{i=1}^{m}\left[\frac{1}{n}\sum_{j=1}^{n}\frac{\left|F_{ij,calc} - F_{ij,\exp}\right|}{F_{ij,\exp}}\times 100\right] \quad (4)$$

Where (m) is the number of experimental runs while (n) is the number of lumped components in the reaction network. In this study, the rate equations parameters estimated by decimal genetic algorithm. The schematic procedure was shown in Figure 3. A random set of candidates for pre-exponential factor and activation energy, within the range defined by the operator was selected by software, at the first step of the estimation procedure. Then the OF for each candidate was calculated using MATLAB software. The candidates are known as "population" and its relevant objective function nominated as "chromosome". In present study, a population with 100 chromosomes was chosen. In the next phase, two parents form the population was selected to make the next generation through mating and mutation. This selection process led to a new chromosome called offspring. 50 percent of the previous chromosomes with higher objective function value would be replaced by these offsprings, as recommended by [33]. The parent selection process was done by choosing a percentage of the best individual by applying the elitist method [34, 35]. The mating process was done using the following crossover operator to generate a new offspring from two selected chromosomes of the current generation.

$$offspring_1 = \beta \times Parent_1 + (1-\beta)\times Parent_2 \quad (5)$$

$$offspring_2 = \beta \times Parent_2 + (1-\beta)\times Parent_1 \quad (6)$$

Also, the following mutation operator with a 15% probability was used to modify new offsprings. This operation helps to make a new population for the next generation [20].

$$Mutated.Gen = Original.Gen\times(1-\xi) + \xi\times(a_i - b_i) \quad 7)$$

Where a_i-b_i is a variable range and ξ is a random positive number less than one. After mutations, the objective function associated with the new population was computed and the already discussed procedure was iterated. The genetic algorithm stopped when 500 iterations happened without any apparent change in the objective function.

The Evans–Polanyi equation [36] was applied to find

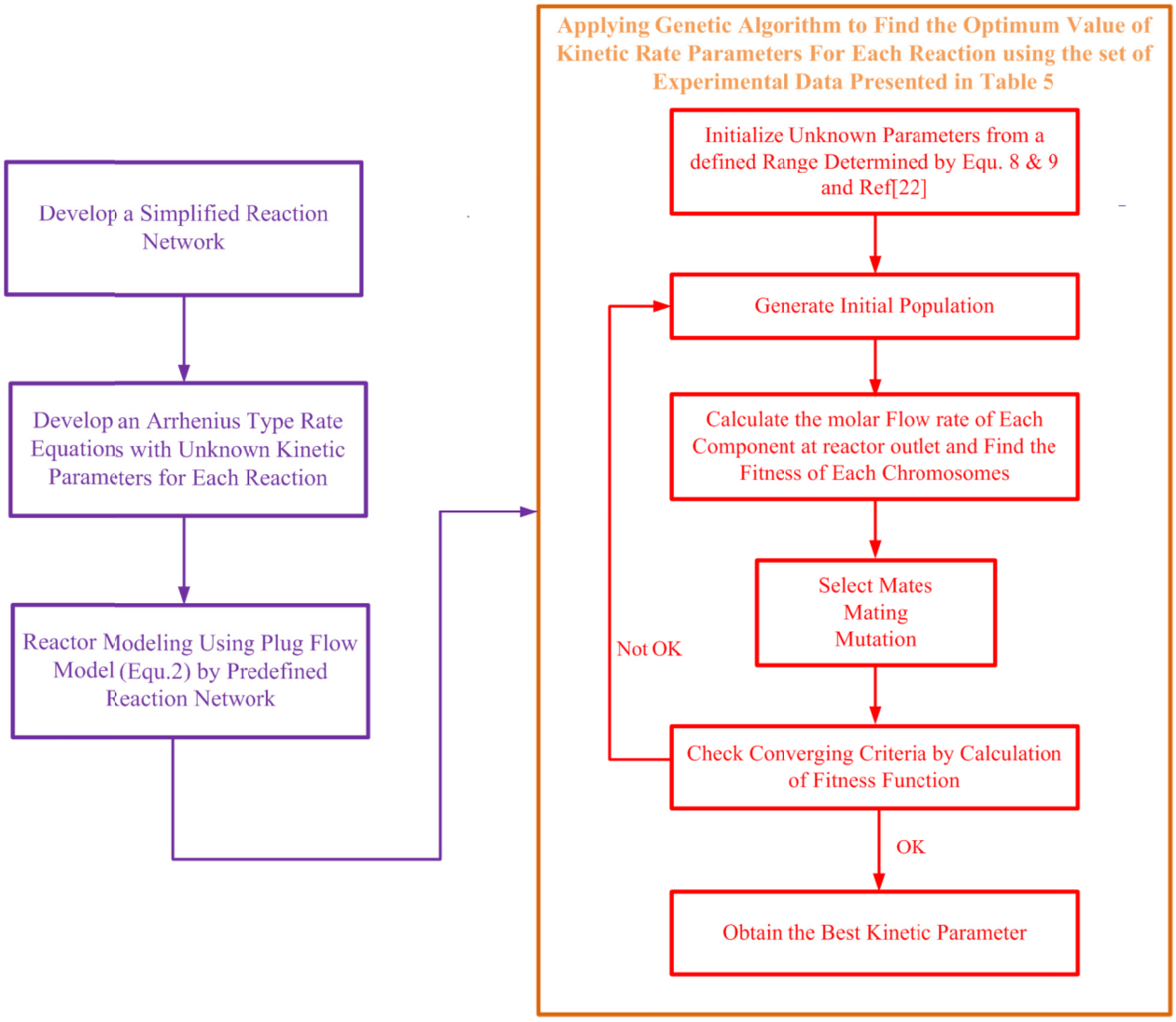

Figure 3. A simplified flowchart for determining MTP reaction network and its kinetic parameters using genetic Algorithm

activation energy initial guesses in generating the first population in the genetic algorithm. This equation related the activation energy to energy released in the reaction and is presented as follows:

$$E_a = E_a^0 - \alpha|\Delta H_r| \quad \text{for exothermic reaction} \qquad (8)$$

$$E_a = E_a^0 - (1-\alpha)|\Delta H_r| \quad \text{for endothermic reaction} \qquad (9)$$

Parameters Value and Results of the proposed model

By considering the experimental data presented in this study, the reaction rates parameters were estimated using the general procedure which was explained in Figure 3. The minimization of the objective function was performed by a written code of the Genetic Algorithm in MATLAB software. The objective function value related to each iteration was depicted in Figure 4. After 3680 iterations the OF reached the value of 11.16, and further try did not lead to better results. The model parameters corresponding to this global minimum were shown in Table 6. Based on the estimated parameters, the flow rates of lower molecular weight olefins, as the main products in the MTP process, were calculated by the reactor model. These data were compared to those gathered from experimental data in the fixed bed reactor and were shown in Figure 5. These parity plots showed reasonable coloration between predicted values and experimental data.

The activation energy associated with the reaction of ethylene production from methanol (E_3) is higher than the value associated with the ethylene production reaction from DME (E_2). Therefore, ethylene mainly

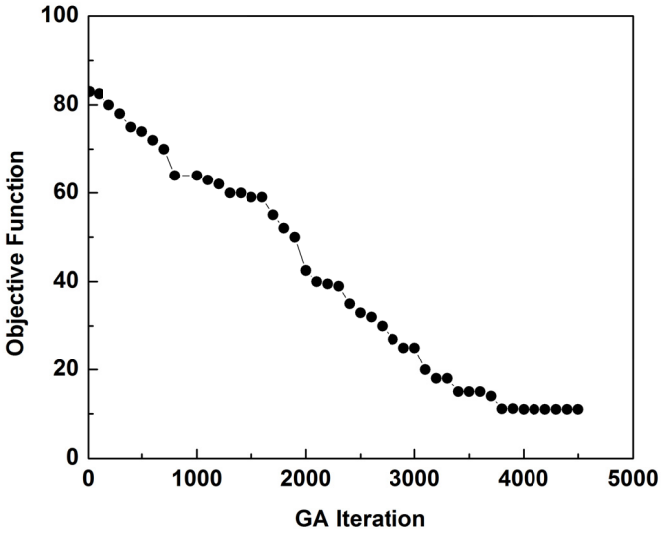

Figure 4. The objective function value versus GA iteration during estimation of the kinetic parameters of MTP reaction network on Ce-H-SAPO-34 Catalyst

Table 6. The kinetic coefficients of the MTP process

Reaction	K_{0j}	E_j
$r_1 = k_{01}.\exp(-\frac{E_1}{RT}).C_{MeOH}{}^2 - \frac{k_{01}}{K}.\exp(-\frac{E_1}{RT}).C_{DME}.C_{H_2O}$	3.2×10^5	**73.2**
$r_2 = k_{02}.\exp(-\frac{E_2}{RT}).C_{DME}$	1.2×10^6	**65.1**
$r_3 = k_{03}.\exp(-\frac{E_3}{RT}).C_{MeOH}$	2.6×10^6	**103.2**
$r_4 = k_{04}.\exp\left(-\frac{E_4}{RT}\right).C_{DME}.C_{C_2H_4}$	2.3×10^5	**55.1**
$r_5 = k_{05}.\exp\left(-\frac{E_4}{RT}\right).C_{MeOH}.C_{C_2H_4}$	3.4×10^5	**43.9**
$r_6 = k_{06}.\exp\left(-\frac{E_6}{RT}\right).C_{DME}.C_{C_3H_6}$	2.1×10^6	**76.1**
$r_7 = k_{07}.\exp\left(-\frac{E_7}{RT}\right).C_{MeOH}.C_{C_3H_6}$	2.6×10^6	**65.7**
$r_8 = k_{08}.\exp\left(-\frac{E_8}{RT}\right).C_{DME}.C_{C_4H_8}$	3.1×10^6	**87.4**
$r_9 = k_{09}.\exp(-\frac{E_9}{RT}).C_{MeOH}$	1.6×10^6	**125.3**
$r_{10} = k_{010}.\exp\left(-\frac{E_{10}}{RT}\right).C_{CO}.C_{H_2O}$	2×10^6	**121.1**
$r_{11} = k_{11}.\exp\left(-\frac{E_{11}}{RT}\right).C_{MeOH}.C_{H_2}$	1.2×10^6	**116.5**
$r_{12} = k_{012}.\exp\left(-\frac{E_{12}}{RT}\right).C_{C_2H_4}.C_{H_2}$	1.6×10^6	**122.1**
$\boldsymbol{Note1: if\ j = 2,3\ [k_{0j}] = \frac{m^3}{gr.hr}}$ $\boldsymbol{for\ other\ [k_{0j}] = \frac{(m^3)^2}{gr.mol.hr}}$		
$\boldsymbol{Note2: [E_j] = \frac{kJ}{mol}}$		

produced from DME at a lower temperature. As temperature rises to higher values, ethylene primarily produced from methanol. As a result, the ethylene produced at lower temperatures is more likely react with methanol in the hydrocarbon pool inside the Hierarchical pores. In comparison with the kinetic data reported by Taheri Najafabadi et al. [22] on conventional SAPO-34, the activation energy for the

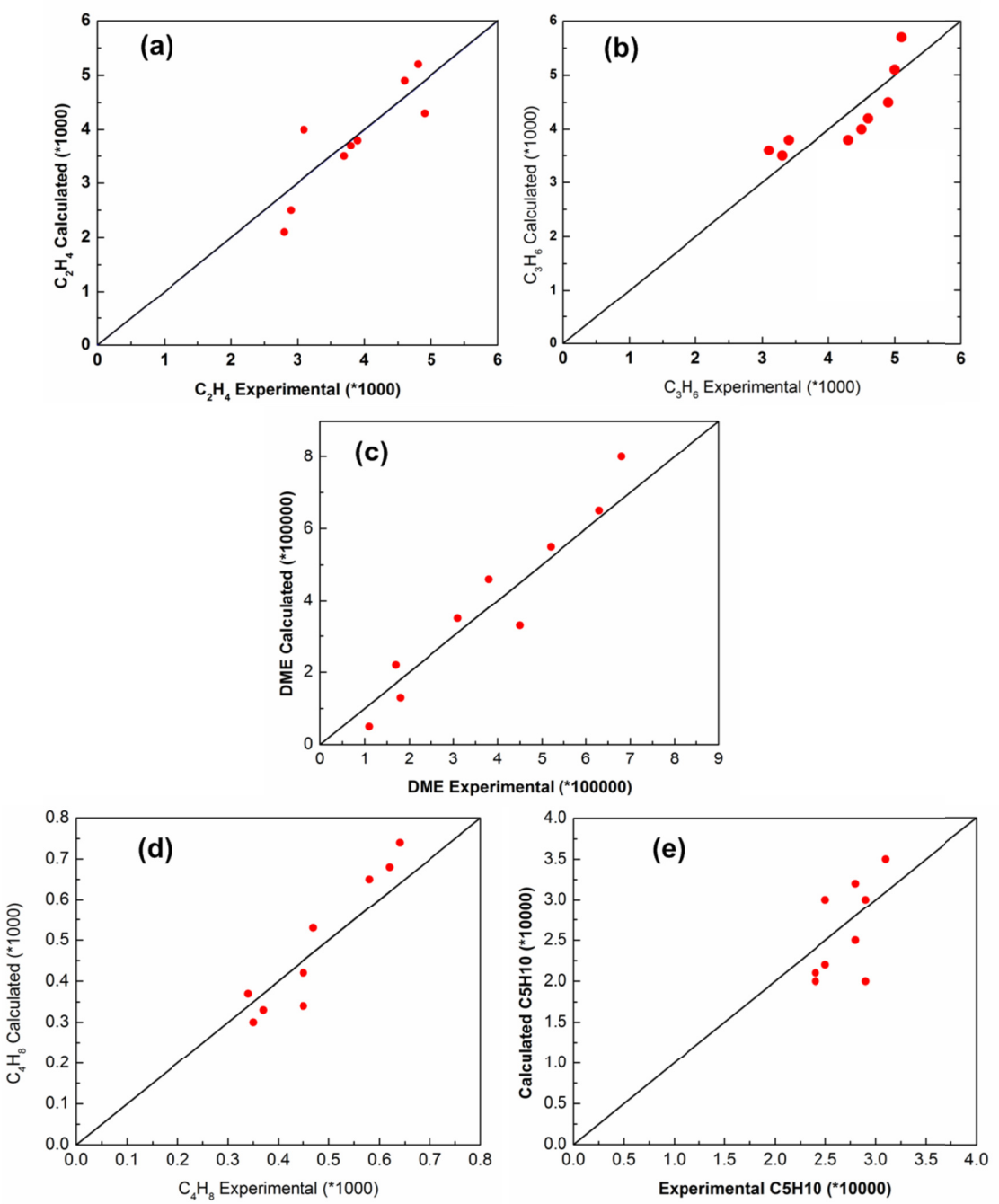

Figure 5. Experimental and calculated Flow rates of (a)ethylene, (b)propylene, (c) Dimethyl ether, (d)Butene and (e) Pentene on Ce-H-SAPO-34 catalyst at reactor outlet.

production of saturated hydrocarbons has been increased in the present work, which is fully consistent with laboratory data. Therefore, the selectivity toward valuable olefins were higher for Ce-H-SAPO-34 catalyst rather than conventional SAPO-34.

To examine the suggested reaction network in present work and the related kinetic model capability, the performance of an experimental fixed bed reactor was predicted. 1 g of Ce-H-SAPO-34 catalyst was loaded in the reactor while a flow of methanol/water mixture passed through the bed with WHSV = 1 h^{-1} at 450 °C. The detailed results of this MTP process were reported by [14]. The comparative results are summarized in Table 7. As is clear, the kinetic model

Table 7. The difference between predicted data obtained from proposed model and experimental data reported data by [14].

Selectivity	Model	Experiment	Relative error (%)
Ethylene	9.6	10.2	-5.9
Propylene	52.2	52.5	-1.1
Butylenes	23.4	22.5	4.0

proposed in this work, is good enough to anticipate the product distribution and performance of fixed bed catalytic reactor of methanol to propylene process.

Conclusion

In the present study, Cerium promoted hierarchical SAPO-34 nanostructure was prepared by the sequence of hydrothermal and impregnation methods. A novel lumped kinetic model was developed for MTP reaction on Ce-H-SAPO-34 catalyst based on surface characteristics of this catalyst regarding to conventional SAPO-34 catalyst. The reaction rate kinetic parameters of the proposed model were estimated using genetic algorithm. The parity plots showed reasonable coloration between predicted values of this new reaction network and experimental data of the fixed bed reactor. So, the reaction network and the related kinetic model suggested in present work could forecast the performance of the MTP process.

References

1. Feng R., Yan X., Hu X., Zhang Y., Wu J., Yan Z. The effect of co-feeding ethanol on a methanol to propylene (MTP) reaction over a commercial MTP catalyst. *Appl. Catal. A*., **599**: 117429 (2020).
2. Rami M. D., Taghizadeh M., Akhoundzadeh H. Synthesis and characterization of nano-sized hierarchical porous AuSAPO-34 catalyst for MTO reaction: Special insight on the influence of TX-100 as a cheap and green surfactant. *Microporous Mesoporous Mater.* **285**(1):259-270 (2019).
3. Shang Y., Wang W., Zhai Y., Song Y., Zhao X., Ma T., Wei J., Gong Y. Seed-fused ZSM-5 nanosheet as a superior MTP catalyst: synergy of micro/mesopore and inter/external acidity. *Microporous Mesoporous Mater.* **276** (1):173-82 (2019).
4. Hu H., Cao F., Ying W., Sun Q., Fang D. Study of coke behaviour of catalyst during methanol-to-olefins process based on a special TGA reactor. *Chem. Eng. J.* **160**(2):770-8 (2010).
5. Bjørgen M., Svelle S., Joensen F., Nerlov J., Kolboe S., Bonino F., et al. Conversion of methanol to hydrocarbons over zeolite H-ZSM-5:On the origin of the olefinic species. *J. Catal.* **249**(2):195-207(2007).
6. Hu Z., Zhang H., Wang L., Zhang H., Zhang Y., Xu H., et al. Highly stable boron-modified hierarchical nanocrystalline ZSM-5 zeolite for the methanol to propylene reaction. *Catal Sci Technol.* **4** (9):2891-5(2014).
7. Sun X., Mueller S., Liu Y., Shi H., Haller G.L., Sanchez-Sanchez M., et al. On reaction pathways in the conversion of methanol to hydrocarbons on HZSM-5. *J. Catal.* **317**:185-97(2014).
8. Li Z., Martínez-Triguero J., Yu J., Corma A. Conversion of methanol to olefins: Stabilization of nanosized SAPO-34 by hydrothermal treatment. *J. Catal.* **329**:379-88 (2015).
9. Dubois D.R., Obrzut D.L., Liu J., Thundimadathil J., Adekkanattu P.M., Guin J.A., et al. Conversion of methanol to olefins over cobalt-, manganese-and nickel-incorporated SAPO-34 molecular sieves. *Fuel Process. Technol.* **83**(1-3):203-18(2003).
10. Wu L., Hensen E.J. Comparison of mesoporous SSZ-13 and SAPO-34 zeolite catalysts for the methanol-to-olefins reaction. *Catal. Today.* **235**:160-8(2014).
11 . Sun Q., Wang N., Xi D., Yang M., Yu J. Organosilane surfactant-directed synthesis of hierarchical porous SAPO-34 catalysts with excellent MTO performance. *Chem Commun.* **50**(49):6502-5(2014).
12. Xi D., Sun Q., Xu J., Cho M., Cho H.S., Asahina S., et al. In situ growth-etching approach to the preparation of hierarchically macroporous zeolites with high MTO catalytic activity and selectivity. *J. Mater. Chem. A*. **2** (42):17994-8004 (2014).
13.Ghalbi-Ahangari M., Rashidi-Ranjbar P., Rashidi A., Teymuri M. Synthesis of hierarchical SAPO-34 and its enhanced catalytic performance in methanol to propylene conversion process. *Pet. Sci. Technol*. **37**(22):2231-7(2019).
14. Ghalbi-Ahangari M., Ranjbar P.R., Rashidi A., Teymuri M. The high selectivity of Ce hierarchical SAPO-34 nanocatalyst for the methanol to propylene conversion process. *React Kinet. Mech. Catal*. 122(2):1265-79 (2017).
15. Huang F., Cao J., Wang L., Wang X., Liu F. Enhanced catalytic behavior for methanol to lower olefins over SAPO-34 composited with ZrO_2. *Chem. Eng. J.*; **380**:122626(2020).
16. Yuan X., Li H., Ye M., Liu Z. Comparative study of MTO kinetics over SAPO-34 catalyst in fixed and fluidized bed reactors. *Chem. Eng. J.* **329** (1):35-44(2017).
17. Lesthaeghe D., Delcour G., Van-Speybroeck V., Marin G.B., Waroquier M. Theoretical study on the alteration of fundamental zeolite properties by methylene functionalization. *Microporous. Mesoporous. Mater*, **96** (1-3):350-356 (2006).
18. Hadi N., Niaei A., Nabavi S.R., Farzi A. Kinetic Study of Methanol to Propylene Processon High Silica H-ZSM5 Catalyst. *IRAN. J. CHEM. CHEM. ENG.* **4**(10): 16-27 (2013).
19. Olsbye U., Bjørgen M., Svelle S., K. Lillerud P., Kolboe S. Mechanistic insight into the methanol-to-

hydrocarbons reaction. *Catal. Today,* **106** (1-4): 108-111 (2005).

20. Gayubo A.G., Aguayo A.T., Alonso A., Bilbao J. Kinetic modeling of the methanol-to-olefins process on a silicoaluminophosphate (SAPO-18) catalyst by considering deactivation and the formation of individual olefins. *Ind. Eng. Chem. Res,* **46**(7):1981-9(2007).
21. Aguayo A.T., Mier D., Gayubo A.G., Gamero M., Bilbao J. Kinetics of methanol transformation into hydrocarbons on a HZSM-5 zeolite catalyst at high temperature (400−550 C). *Ind. Eng. Chem. Res,* **49**(24):12371-8(2010).
22. Najafabadi A.T., Fatemi S., Sohrabi M. Kinetic modeling and optimization of the operating condition of MTO process on SAPO-34 catalyst. *J. Ind. Eng. Chem,* **18** (1), 29-37 (2012).
23. Treacy M.M.J., Higgins J.B. Collection of Simulated XRD Powder Patterns for Zeolites, 4th Structure Commission of the International Zeolite Association. *Amsterdam, Netherlands*. p 380, (2001).
24. Shamanaeva I., V. Parkhomchuk E. Influence of the Precursor Preparation Procedure on the Physicochemical Properties of Silicoaluminophosphate SAPO-11. *Pet.Chem*. **59**(8): 854-859 (2019).
25. Li J., Li Z., Han D., Wu J. Facile synthesis of SAPO-34 with small crystal size for conversion of methanol to olefins. *Powder Technol,* **262**: 177-182 (2014).
26. Gayubo A.G., guayo A. T., Sánchez A.E. Kinetic Modeling of Methanol Transformation into Olefins on a SAPO-34 Catalyst. *Ind. Eng. Chem. Res,* **39** (2): 292-301 (2000).
27. Bos A.N.R., Tromp P.J.J., Akse H.N. Conversion of Methanol to Lower Olefins. Kinetic Modeling, Reactor Simulation, and Selection. *Ind. Eng. Chem. Res,* **34**(11): 3808-3818 (1995).
28. Park T.Y., Froment G.F. Kinetic modeling of the methanol to olefins process. 1. Model formulation. *Ind. Eng. Chem. Res*.;**40** (20):4172-86 (2001).
29. Park T.Y., Froment G.F. Kinetic Modeling of the Methanol to Olefins Process. 2. Experimental Results, Model Discrimination, and Parameter Estimation *Ind. Eng. Chem. Res,* **40**: 4187-4197 (2001).
30. Abraha M.G., Wu X., Anthony R.G. Effects of particle size and modified SAPO-34 on conversion of methanol to light olefins and dimethyl ether. *Stud. Surf. Sci. Catal.* **133**: Elsevier; 2 11 – 218(2001).
31. Daneshpayeh M., Khodadadi A., Mostoufi N., Mortazavi Y., Sotudeh-Gharebagh R., Talebizadeh A. Kinetic modeling of oxidative coupling of methane over $Mn/Na_2WO_4/SiO_2$ catalyst. *Fuel. Process. Technol*. **90**(3):403-410 (2009).
32. Alwahabi S.M., Froment G.F. Single event kinetic modeling of the methanol-to-olefins process on SAPO-34. Ind. *Eng. Chem. Res.* **43**(17):5098-111(2004).
33. Maeder M., Neuhold Y.M., Puxty G. Application of a genetic algorithm: near optimal estimation of the rate and equilibrium constants of complex reaction mechanisms. *Chemom. Intell. Lab. Syst., Lab. Inf. Manage*. **70** (2): 193-203 (2004).
34. Lucasius C.B., Kateman G. Understanding and using genetic algorithms Part 2. Representation, configuration and hybridization. *Chemom. Intell. Lab. Syst.* **25**: 99-145 (1994).
35. Maeder M. , Neuhold Y. M., Puxty G., King P. Analysis of reactions in aqueous solution at non-constant pH: no more buffers?. *Phys. Chem. Chem. Phys*. **5:** 2836-2841 (2003)
36. Evans M., Polanyi M. Inertia and driving force of chemical reactions. *Trans. Faraday Soc,* **34**: 11-24 (1938).